Entropy of the quantum soliton lattice and multiple magnetization steps in BiCu_{2}PO_{6}

Yoshimitsu Kohama, Kenji Mochidzuki, Taku Terashima, Atsuhiko Miyata, Albin DeMuer, Thierry Klein, Christophe Marcenat, Z. L. Dun, Haidong Zhou, Gang Li, Luis Balicas, Nozomu Abe, Yasuhiro H. Matsuda, Shojiro Takeyama, Akira Matsuo, and Koichi Kindo

Phys. Rev. B **90**, 060408 — Published 25 August 2014

DOI: 10.1103/PhysRevB.90.060408

Entropy of the Quantum Soliton Lattice and Multiple Magnetization Steps in $BiCu_2PO_6$

Yoshimitsu Kohama,[1] Kenji Mochidzuki,[1] Taku Terashima,[1] Atsuhiko Miyata,[1] Albin DeMuer,[2] Thierry Klein,[3,4] Christophe Marcenat,[5] Z. L. Dun,[6] Haidong Zhou,[6,7] Gang Li,[7] Luis Balicas,[7] Nozomu Abe,[1] Yasuhiro H. Matsuda,[1] Shojiro Takeyama,[1] Akira Matsuo,[1] and Koichi Kindo[1]

[1] *ISSP, University of Tokyo, Kashiwa, Chiba 277-8581, Japan*
[2] *LNCMI, CNRS-Université de Grenoble Joseph Fourier, Grenoble, France*
[3] *Univ. Grenoble Alpes, Institut Néel, F-38000 Grenoble, France*
[4] *CNRS, Institut Néel, Grenoble F-38042, France*
[5] *SPSMS, UMR-E9001, CEA-INAC/UJF-Grenoble 1, 17 rue des Martyrs, Grenoble 38054, France*
[6] *Department of Physics and Astronomy, University of Tennessee, Knoxville, Tennessee 37996-1200, USA*
[7] *NHMFL, East Paul Dirac Drive, Tallahassee, Florida 32310, USA*

$BiCu_2PO_6$, a spin gapped material in a frustrated two-leg ladder lattice, exhibits a complex (H,T) phase diagram in external magnetic fields. We have characterized the field-induced phases through specific heat, magnetocaloric effect, Faraday rotation, and magnetization measurements in fields up to 120 T. In addition to observing a new magnetic phase above 60 T which we attribute to the crystallization of triplet excitations, our measurements reveal the emergence and the subsequent disappearance of a high entropy (short-range ordered) phase at a first- and second-critical magnetic field, respectively. This is in a good agreement with the theoretical prediction of a quantum soliton lattice at intermediate fields.

A spin gap opens in many different quantum magnets, such as spin-dimers, frustrated chains, even-leg spin ladders. In many cases, the ground state is a singlet, with the excited one being a triplet band at higher energies. Application of a magnetic field closes the spin gap at a first critical field (H_{c1}) where the minimum of the triplet band crosses the singlet state. Depending on the spin Hamiltonian describing the system, above H_{c1}, different types of field-induced (FI) phases can arise as a result of a triplet condensation, including a Mott-insulating state with a superlattice order [1,2], a Bose-Einstein condensate [3], or a supersolid [4]. In frustrated magnets with a degenerate ground state, a further increase in magnetic field strength towards a second critical value (H_{c2}) triggers a transition to another exotic FI phase. Such a cascade of FI phase-transitions can occur at several critical fields (H_{c3}, H_{c4}, …, H_{sat}) until the magnetic moment is fully saturated.

$BiCu_2PO_6$, a frustrated two-leg ladder, is a material in which a cascade of FI transitions is observed [5]. Based on the experimental observations, the formation of an exotic *soliton lattice* was suggested when the high magnetic field is applied along the *b*-axis [6]. This phase is located at the edge of a dome-shaped phase diagram and here we denominate it as Phase II_b (see Fig. 1). A theoretical model proposes that the solitonic phase results from magnetic frustration and is quite different from a classical soliton lattice in spin-Peierls systems in which the spin-lattice coupling plays an important role [7]. Theoretically, the soliton lattice in $BiCu_2PO_6$ results from the crystallization of a $S = 1/2$ effective spin arising from the fractionalization of the $S = 1$ triplet excitations [6]. The triplet picture is predicted to become relevant above H_{c2}, and $BiCu_2PO_6$ might be the only compound exhibiting a sequence of FI phases from a $S = 1/2$ soliton lattice to a $S = 1$ triplet condensate as the field increases. However, since the measurements at high magnetic fields are experimentally challenging, detailed investigations remain scarce. To date, no experiment has been performed above 60 T, although the emergence of a novel ground state can be expected when increasing the field up to $H_{sat} \sim 500$ T [8], the value in field required to saturate the magnetization. Furthermore, for $H \parallel a$, the determination of the (H, T) phase diagram remains incomplete.

Here, we report a complete set of measurements in $BiCu_2PO_6$, including magnetocaloric effect (MCE), specific heat (C_p), magnetization (M), and Faraday rotation (Θ_M) in magnetic fields up to 120 T. From the MCE and C_p measurements, we reveal the evolution of the magnetic entropy and of the magnetic phase diagram for magnetic fields applied along all three crystallographic axes, as summarized in Fig. 1. We find an evidence for a soliton phase (Phase II_b) characterized by high entropy due to

short-range spin-spin ordering, which subsequently is observed to disappear when entering Phase III_b. This finding is in line with a recent study suggesting the formation and the collapse of a soliton lattice [6]. Faraday rotation and magnetization measurements unveil the further occurrence of another FI transition for fields above 60 T, which we claim could correspond to a triplet condensate such as a magnetic superstructure, or even a supersolid phase.

Single crystals of $BiCu_2PO_6$ were grown at the National High Magnetic Field Laboratory and at the University of Tennessee by the floating zone technique [9]. In this material, the $S = 1/2$ magnetic moments of the Cu^{2+} ions are arranged in a zigzag shaped ladder along the *b*-axis. The structure leads to frustrated interactions between the leg coupling ($J_{Leg} \sim 140$ K) and the Next-nearest-neighbor coupling ($J_{NNN} \sim 140$ K) [10]. Along the rung direction (*c*-axis), the Cu-O-Cu super-exchange interaction leads to the rung coupling ($J_{Rung} \sim 3J_{Leg}/4$). The ladder units are weakly coupled along the rung direction and form magnetically interacting *bc* planes. These planes are stacked along the *a*-axis with negligible magnetic interactions.

Figure 1 presents the (*H,T*) phase diagram for $BiCu_2PO_6$. The phase boundaries depicted by open triangles and circles were determined by C_p and MCE measurements, respectively, while the phase boundaries reported in Ref.5 were plotted as dots. The field dependence of C_p was collected in a 36 T long pulse magnet (1 s pulse duration) by using an AC technique [11] which is shown in Fig. 2(a). The temperature dependence of the specific heat was measured under both a 34 T static and a 60 T short pulsed magnet (36 ms pulse duration). By subtracting the lattice contribution (C_{lat}) as determined from its nonmagnetic analog $BiZn_2PO_6$ [13], we obtained the magnetic contribution to the specific heat (C_M) and plotted it as $C_M T^{-1}$ in Fig. 2(b). The data taken in a short pulsed magnet (solid squares in Fig.2(b)) were collected by using the heat pulse technique [12]. Although this technique allows the study of thermodynamic properties in pulsed magnetic fields, it comes at the cost of reduced accuracy. Thus, data were also collected below 34 T under static fields (curves in Fig.2 (b)) to confirm the quality of the C_p measurements under pulsed fields. For these specific heat measurements, the field was applied parallel to the *a*-axis.

Figure 2(a) shows C_p as a function of H at different temperatures. At 2.5 K, a sharp cusp is observed around $H_{c1} \sim 24$ T which moves to higher fields as T increases. Adding to this phase-transition, these data show a sequence of phase-transitions with a hysteretic feature at $H_{c2} \sim 30$ T. A remarkable hysteresis, the signature for a 1^{st} order phase-transition, is also observed in the MCE (red curve in Fig. 3(a)) and in the magnetization (inset of Fig. 4(a)). Because of the agreement among the C_p, M, and MCE

measurements, we conclude that a 1st order phase-transition occurs at H_{c2} ~ 30 T when the magnetic field is applied along the *a*-axis. From the temperature at which the peak in $C_M T^{-1}$ is observed in Fig. 2(b), we also determined the phase boundaries.

To obtain additional thermodynamic information, MCE measurements under adiabatic conditions[14] were performed in pulsed magnetic fields up to 56.5 T for fields applied along the *a*, *b*, and the *c*-axes. The black curves in Fig. 3(a) are selected MCE data for *H*//*b,* in which the phase boundaries are deduced from kinks in the MCE traces (superimposed as open circles). In the low-field spin gapped phase (Phase I_b), the MCE curves show a gradual decrease in temperature towards the first phase boundary. Above this boundary (Phase II_b), a plateau is visible in the $T(H)$ curve. After reaching the second phase boundary (Phase III_b), $T(H)$ shows a sudden increase. Noteworthy, when the magnetic field is applied along the *a*- (red) or the *c*-axis (blue), $T(H)$ does not show any plateau and becomes hysteretic. This suggests that while the FI transition for *H*//*b* is second-order in nature, the transitions for *H*//*a* and *c* behave like first-order transitions.

The MCE traces in Fig. 3(a) were measured under adiabatic conditions. Thus, the reversible MCE curves correspond to isoentropic temperature changes as a function of the magnetic field, *i.e.*, the entropy remains constant when collecting reversible $T(H)$ curves [14]. Although there is an irreversible region in $T(H)$ around the 1st order phase boundaries, it only induces negligible errors, *i.e.* ~0.3 K, due to the small size of the hysteresis. Hence, we used the MCE data corresponding to field-down sweeps to estimate the magnetic entropy (S_M) at high magnetic fields. The resulting $T(H,S_M)$ is shown in Figs. 1(a-c) as color contour plots. The Phase I is a spin-gapped phase and contains low entropy when compared to the FI phases (Phase II, III, … V). The anomaly in $S_M(T,H)$ is also evident at the phase boundaries.

For the sake of a detailed comparison of the entropy among the data obtained for all three field orientations, we extracted the field dependence of S_M at constant temperatures which is shown in Fig. 3(b). Here, arrows indicate the phase boundaries between Phase I and II for *H*//*a* and *b* (or between Phases I and IV for *H*//*c*), respectively. Dotted arrows correspond to phase boundaries between Phases II and III (or between IV and V)) for *H*//*a* and //*b* (or //*c*). Despite the anisotropic nature of the phase boundaries, we find that the $S_M(H)$ data in the spin gapped phase (Phase I) show similar trends regardless of the orientation of the applied field. As one approaches the phase boundary from the spin gapped phase at a constant temperature, one observes a clear increase in S_M. This behavior is attributed to an increase in singlet to triplet excitations associated with a reduction in the spin gap as the *H* increases. In other words, an increase in the

number of the thermally excited (disorderd) triplet excitations results in an enhancement of the entropy. Subsequently, in the intermediate field range (Phase II for H//a and b, and Phase IV for H//c), FI phases are observed with the shape of $S_M(H)$ depending on the orientation of the applied field. Within the FI phase(s), the density of spin excitations still increase (the total number of spin excitations can be estimated as being proportional to the uniform magnetization which increases monotonically as a function of H), but their ordering within the FI phase leads to the suppression of the entropy. Indeed, for both H//a and c $S_M(H)$ is suppressed by the emergence of FI spin ordering. This tendency resembles the one observed at the transition from a spin gapped state to the long-range ordered XY antiferromagnetic phase [15]. In contrast, when the magnetic field is applied along the b-axis, $S_M(H)$ shows a plateau which maintains its high entropy within Phase II_b. Eventually, as the field is further increased, another FI phase emerges. As seen in the $S_M(H)$ trace collected at T = 7 K, above 40 T there is a clear reduction in $S_M(H)$ for H//b, indicating the emergence of a phase with a higher degree of spin ordering.

Let us briefly discuss the implications of our $S_M(H)$ data. Recent NMR experiments by F. Casola *et al.* suggested that $BiCu_2PO_6$ forms a quantum soliton lattice in Phase II_b. Their density-matrix renormalization group analysis predicted that the soliton lattice is accompanied by the formation of short-ranged dimer order [6], and that by increasing the magnetic field above H_{c2} one can induce long-range magnetic order (i. e. a canted spin helix). Our finding of a high entropy one transitioning into a low-entropy phase at H_{c2}, is consistent with their model (transition from short-ranged dimer order to long-range order). Our data further indicate that such a high entropy state is not observed for all the different field orientations (H//a or c) in the range of temperatures of our measurements. Indeed, the hysteretic (1^{st} order) nature observed for H//a and //c (MCE in Fig. 3(a)) is inconsistent with the prediction for a soliton lattice.[6] On the other hand, for H//b, Phase II_b is observed over a wide range of temperatures and magnetic fields which offering an ideal playground to investigate the nature of the FI soliton lattice.

It was reported that the magnetic excitations above H_{c2} ~ 34 T can be described within a hard-core Bosonic picture (i. e. triplet excitations)[6]. In materials that possess both strong frustration and triplet excitations, the application of a magnetic field can induce a cascade of triplet condensates, as reported for $SrCu_2(BO_3)_2$ [4]. To explore the magnetic phase diagram under higher magnetic fields, we now turn to different observables, magnetization (M) and the Faraday rotation angle (Θ_M), which are the available experimental techniques for ultrahigh magnetic fields, i.e. exceeding ~100 T.

M was measured at ~ 2 K with the samples immersed in liquid ^{4}He, and Θ_M was measured at different temperatures by using a flow-type cryostat. Both measurements were performed in a single turn coil (10 μs pulse duration) up to 120 T. In addition, M was also measured in a 75 T non-destructive magnet at 1.5 K (4 ms pulse duration). The details of the M and the Θ_M measurements were described elsewhere [4,16,17]. To the best of our knowledge, this is the first investigation of $BiCu_2PO_6$ in fields up to 120 T, higher than in any of the previous studies.

The $M(H)$ data shown in Fig. 4(a) exhibit three new features. (i) As shown in the inset of Fig. 4(a), we observe a hysteretic jump at 30 T for $H//a$, indicating a first-order phase-transition at H_{c2} ~ 30 T. (ii) For H // a, we observe additional weak anomalies in fields exceeding 60 T; a kink and a shoulder in M at ~65 and 80 T (red arrows) respectively, indicating yet further FI transitions. This finding is also supported by the Θ_M measurements as a function of H (Fig. 4(b)). While $\Theta_M(H)$ at 16 K shows paramagnetic response, *i.e.* linear in H, at 10 K and 65 T it exhibits a concave down curvature increasing again above 90 T. Although Θ_M and M were measured at different temperatures, lines depicting the phase boundaries in the phase diagram tend to be nearly vertical for $H//a$ (Fig. 1(a)). Therefore, both the Θ_M and the M measurements seem to detect the same phase boundaries. (iii) When the magnetic field is applied along the b-axis, a broad shoulder in M is evident at 80 T (indicated by a black arrow). For $H//c$, M shows an upturn at 75 T (blue arrow). Although we observe a strongly anisotropic magnetization, the sequence of FI transitions continues above 60 T, regardless of field orientation.

Considering that repulsive interactions between triplets tend to be dominant in a frustrated quantum magnet, an incompressible superstructure such as a triplet superlattice or a supersolid phase, can be a plausible candidate for the high field FI-phases. An early theoretical study predicts only one anomaly in $M(H)$ at $0.5H_{sat}$ ~ 250 T,[8] and obviously more theoretical calculations as well as experiments are needed to gain a quantitative understanding of the observed high-field phases in $BiCu_2PO_6$.

In summary, we reported measurements of specific heat (C_p), magneto-caloric effect (MCE), Faraday angle (Θ_M), and magnetization (M) in ultrahigh magnetic fields up to 120 T in $BiCu_2PO_6$. Θ_M and M provide the first experimental evidence for a new magnetic phase transition above 60 T. C_p and MCE data unveil the magnetic phase diagram for $H//a$ and allow us to track the evolution of the magnetic entropy. For magnetic fields applied along the b-axis, the isothermal entropy exhibits a remarkable plateau in Phase II_b, but it is suppressed when entering Phase III_b. We argue, based on previous density-matrix renormalization group analysis, that the formation and

collapse of a soliton lattice results in the distinct change in $S(H)$.

Acknowledgements

We acknowledge A. Feiguin for fruitful discussions and Y. Aida for help during experiments. This work was supported by JSPS Grant-in-Aid for Young Scientists (B) Grant Number 25800187. Z. L. D. and H. D. Z. are supported by NSF-DMR through award DMR-1350002. L. B. is supported by DOE-BES through award DE-SC0002613.

References

[1] H. Kodama, M. Takigawa, M. Horvatić, C. Berthier, H. Kageyama, Y. Ueda, S. Miyahara, F. Becca, F. Mila, *Science* **298**, 395 (2002).

[2] T. M. Rice, *Science* **298**, 760 (2002).

[3] Ch. Rüegg, N. Cavadini, A. Furrer, H. -U. Güdel, K. Krämer, H. Mutka, A. Wildes, K. Habicht, and P. Corderwisch, *Nature* **423**, 62 (2003).

[4] Y. H. Matsuda, N. Abe, S. Takeyama, H. Kageyama, P. Corboz, A. Honecker, S. R. Manmana, G. R. Foltin, K. P. Schmidt, and F. Mila, *Phys. Rev. Lett.* **111**, 137204 (2013).

[5] Y. Kohama, S.Wang, A. Uchida, K. Prsa, S. Zvyagin, Y. Skourski, R. D. McDonald, L. Balicas, H. M. Ronnow, C. Rüegg, and M. Jaime, *Phys. Rev. Lett.* **109**, 167204 (2012).

[6] F. Casola, T. Shiroka, A. Feiguin, S. Wang, M. S. Grbić, M. Horvatić, S. Krämer, S. mukhopadhyay, K. Conder, C. Berthier, H.-R. Ott, H. M. Ronnow, Ch. Rüegg, and J. Mesot, *Phys. Rev. Lett.* **110**, 187201 (2013).

[7] A. E. Feiguin, J. A. Riera, A. Dobry, and H. A. Ceccatto, *Phys. Rev. B* **56**, 14607 (1997).

[8] A. A. Tsirlin, I. Rousochatzakis, D. Kasinathan, O. Janson, R. Nath, F. Weickert, C. Geibel, A. M. Läuchli, and H. Rosner, *Phys. Rev. B* **82**, 144426 (2010).

[9] S. Wang, E. Pomjakushina, T. Shiroka, G. Deng, N. Nikseresht, Ch. Rüegg, H. M. Rønnow, and K. Conder, *J. Cryst. Growth* **313**, 51 (2010).

[10] K. W. Plumb, Zahra Yamani, M. Matsuda, G. J. Shu, B. Koteswararao, F. C. Chou, and Y.-J. Kim, *Phys. Rev. B* **88**, 024402 (2013).

[11] Y. Kohama, C. Marcenat, T. Klein, and M. Jaime *Rev. Sci. Instrum.* **81**, 104902 (2010).

[12] Y. Kohama, Y. Hashimoto, S. Katsumoto, M. Tokunaga, and K. Kindo, *Meas. Sci. Technol.* **24**, 115005 (2013).

[13] B. Koteswararao, A. V. Mahajan, L. K. Alexander, and J. Bobroff, *J. Phys. Condens. Matter* **22**, 035601 (2010).

[14] T. Kihara, Y. Kohama, Y. Hashimoto, S. Katsumoto, and M. Tokunaga, *Rev. Sci. Instrum.* **84**, 074901 (2013).

[15] A. A. Aczel, Y. Kohama, C. Marcenat, F. Weickert, M. Jaime, O. E. Ayala-Valenzuela, R. D. McDonald, S. D. Selesnic, H. A. Dabkowska, and G. M. Luke, *Phys. Rev. Lett.* **103**, 207203 (2009).

[16] A. Miyata, H. Ueda, Y. Ueda, H. Sawabe, and S. Takeyama, *Phys. Rev. Lett.* **107** 207203 (2011).

[17] S. Takeyama, R. Sakakura, Y. H. Matsuda, A. Miyata, and M. Tokunaga, *J. Phys. Soc. Jpn.* **81** 014702 (2012).

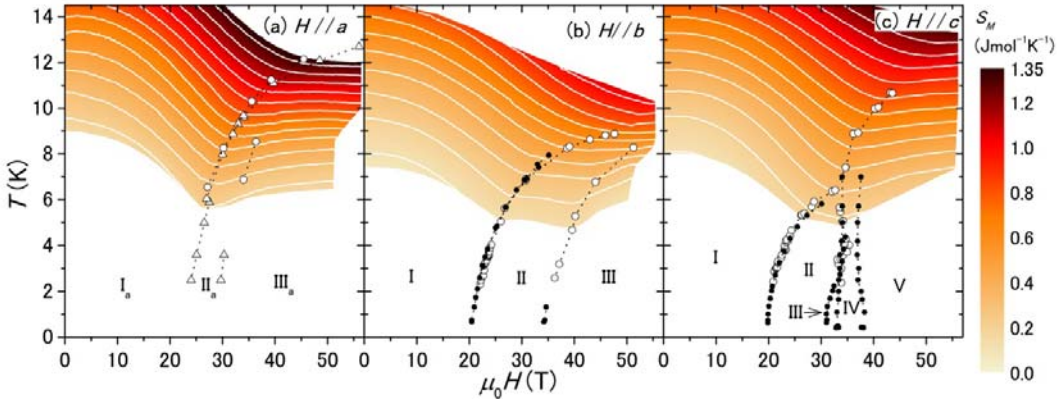

FIG. 1. (a,b,c) Contour map of $S(T,H)$ for $H//a$ (left), $H//b$ (middle), $H//c$ (right). The contour plot of $S_M(T,H)$ is constructed through linear interpolation of a series of $T(H,S_M)$ traces. The phase boundaries determined by MCE and specific heat are also shown as open circles and open triangles, respectively. The solid dots are the phase boundaries reported in Ref. 5. The phase boundaries above 60 T detected by M and Θ_M are not shown for clarity.

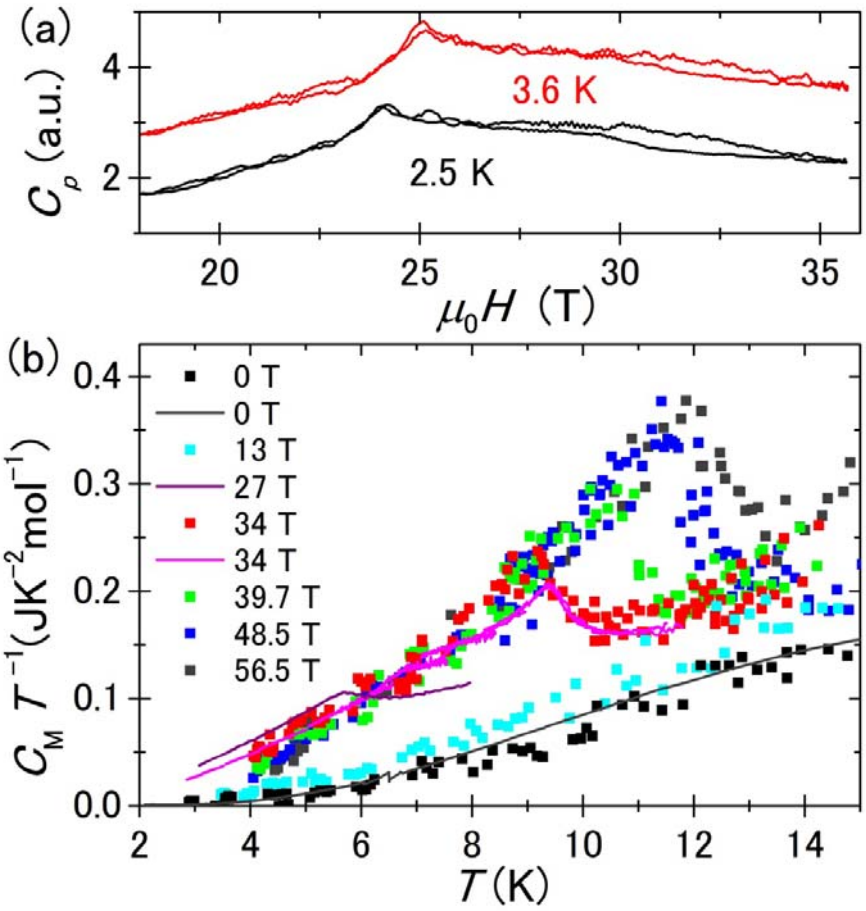

FIG. 2. Specific heat of $BiCu_2PO_6$ for field applied to the *a*-axis. (a) Field dependence of C_p at two temperatures. The results are plotted in arbitrary units. (b) $C_M T^{-1}$ as a function of T as obtained in pulsed magnetic fields (solid squares). Below 34 T, $C_M T^{-1}$ was also collected under static fields (curves).

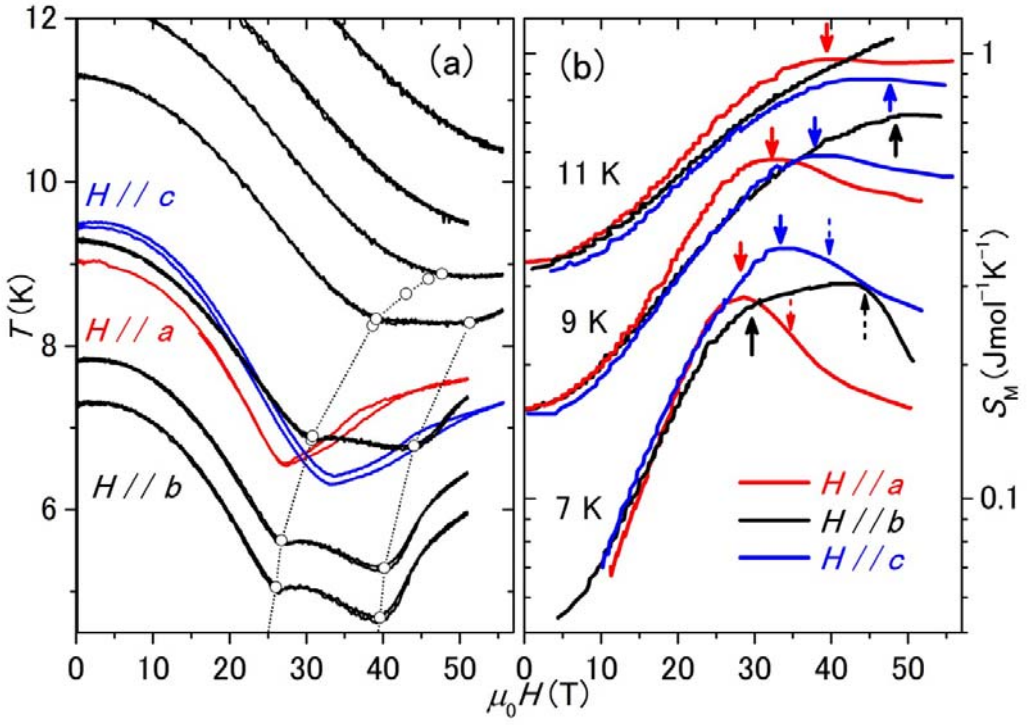

FIG. 3. (a) Selected magneto-caloric effect (MCE) traces measured in the adiabatic condition for $BiCu_2PO_6$. Circles correspond to phase boundaries deduced from MCE experiments. (b) Magnetic entropy (S_M) as a function of H. The solid (dashed) arrows indicate the phase boundaries (see the text). S_M was estimated by subtracting lattice entropy of $BiZn_2PO_6$[13] from the total entropy.

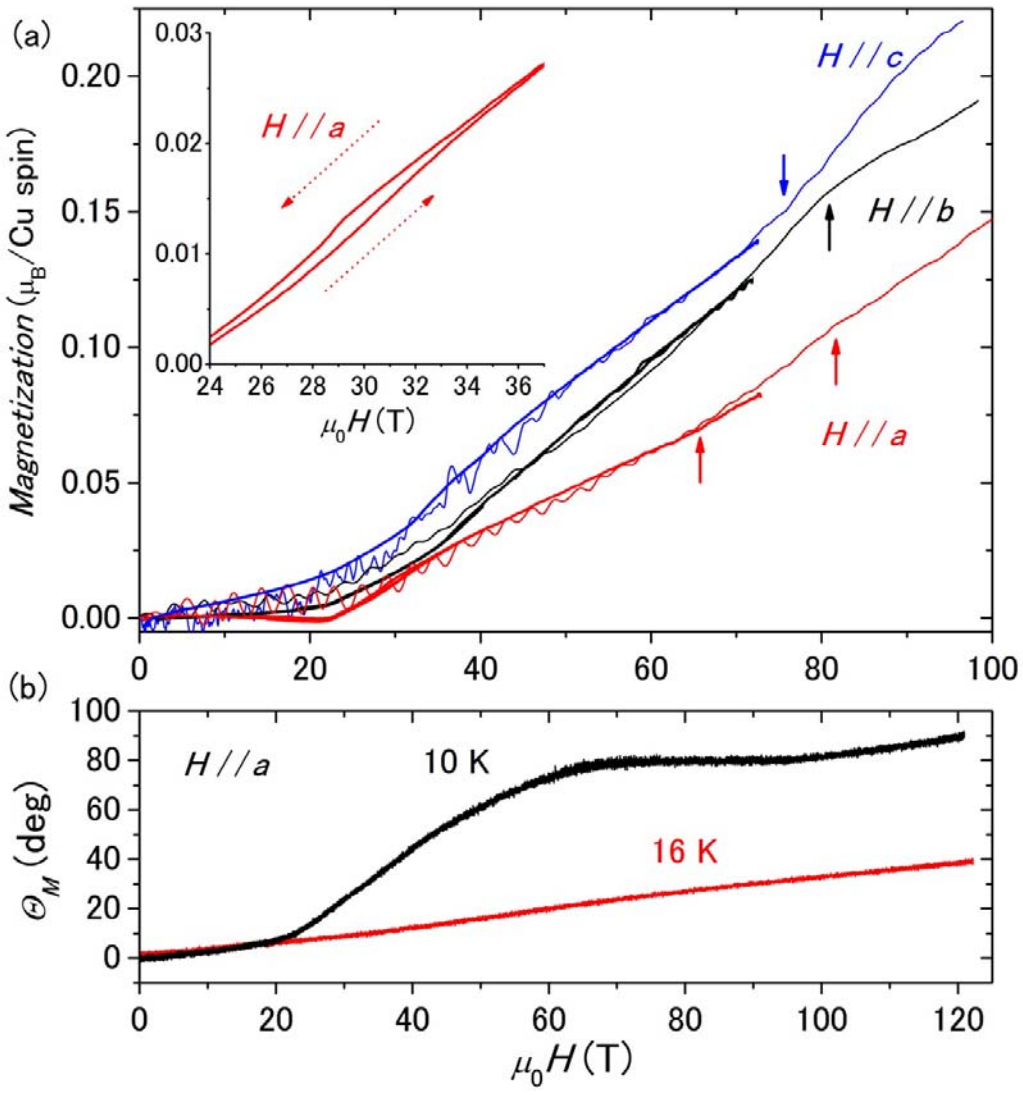

FIG. 4. (a) Magnetization of $BiCu_2PO_6$. Thin curves were obtained in a single turn coil. Thick curves were measured in a 75 T non-destructive magnet. The inset is a magnification showing M as a function of H for H//a. (b) Faraday rotation angle Θ_M at different temperatures. For this measurement, the magnetic field was applied along the a-axis.